Rock Fractures Characterization in the Khairi Murat Range, Sub Himalayan Fold and Thrust Belt, North Pakistan

N. Dasti[1*], S. Akram[1], I. Ahmad[2] and M. Usman[3]

¹Institute of Geology, Punjab University, New Campus, Lahore, Pakistan

²Geological Survey of Pakistan H-8/1, Islamabad, Pakistan

³Department of Mining Engineering, U.E.T, Peshawar, Pakistan

ABSTRACT

The Potwar fold and thrust belt is an area of active oil and gas exploration and production. Fractures are the main contributors toward permeability and enhancing hydrocarbon productivity particularly in carbonates in the region. The migration and accumulation data from the hydrocarbon reservoirs indicate a well-developed fracture system in the area. 2700 individual fractures were measured along 106 scanlines, and 1260 fractures were measured at 27 sample stations using the circle inventory method. 8 fracture sets, named as "set-1" to "set-8" have been identified in the study area. Fracture properties i.e. spacing, aperture, density, porosity and permeability are estimated, which ranges from 8 m^{-1} to 76 m^{-1}, 1.1 cm to 13.4 cm, 0.04 cm^{-1} to 0.22 cm^{-1}, 0.06% to 2.30% and 0.24×10⁸ Darcy to 1446×10⁸ Darcy respectively. A wide range of fracture orientations occurs, creating connected fractures networks. The directional character of connectivity depends upon the direction of the dominant fractures orientation, i.e., NE-SW and NW-SE. The fracture aperture and spacing data show that these parameters statistically follow the Normal and log-Normal distributions respectively. The maximum values of fracture porosity (2.30%), fracture permeability (1446.114×10⁸D) and density (0.217 cm^{-1}) of fractures are related to the vicinity of faults and regionally extended lineaments. Three fracture sets have also been identified and established their relationship with the tectonic stress field in the study area. It is concluded that this study would enhance the data for hydrocarbon production and exploring the groundwater prospects in the area.

1. Introduction

The Khairi Murat Range, about 40km to the southwest of Islamabad is a prominent feature in the structural domain of North Potwar Deformed Zone (NPDZ) and is bound by Main Boundary Thrust (MBT) in the north and Dhurnal Fault (DF) in the south. The area is intensely deformed as a part of Potwar foreland basin where sedimentary strata have been folded and faulted during the Himalayan orogeny. Apart from folding and faulting, a number of other structural elements i.e. lineaments (regional scale structural features), shear zones and fracture swarms developed as a result of Himalayan tectonics are well exposed in the study area [1].

Characterization of rock fractures plays a vital role in understanding the development of petroleum reservoirs, enhancement of their productivity, economical production of geothermal reservoirs, management of groundwater potential and underground nuclear waste repositories [2]. Fracture properties that are important to analyze, include their orientations (dip and strike), aperture and spacing which are important for establishing directional permeability and connectivity of fracture networks [3]. Orientation, spacing and apertures of the fractures are evaluated and characterized in this paper.

Limited research has been carried out on fractures characterization until now in Pakistan. The Khaur anticline in the Central Potwar Plateau has been analyzed by Jadoon et al. [4]. On the Khaur anticline, the iron filled, calcite-filled, quartz filled and open fracture systems have been identified. Open fractures are determined to be the most significant of all other types of fractures and can be used for successful exploration. Fracture porosity and permeability have also been estimated using Monte Carlo techniques. Jadoon et al. [5] worked on the simulation of the fractured reservoir using a single porosity system. The well tests, core analysis and lab testing of non-fractured part of Chorgali Formation through DST showed that single porosity system exists in the Fimkasser reservoir. The matrix porosity ranges from 1% to 3.5% and permeability from 0-0.03 miliDarcy (mD). The Fimkasser oil field was taken as a case study and concluded that a) fractures are more frequently developed in the thin to medium beds as compared to fine-grained thick to massive bedding b) Fimkasser structure is an anticline with a steep eastern flank and c) the fractures of Fimkasser structure are mainly controlled by fold geometry, fault and bed thickness. Jadoon et al. [6] described the involvement of subsurface fractures in carbonate reservoirs in Kohat-Potwar Plateau, reviewed fracture classification and presented a descriptive classification for the subsurface fracture network. A study

---

*Corresponding author :   dastigeo@yahoo.com

of fractures parameters regarding porosity, permeability and connectivity of the fracture network and their role in the productivity of reservoir has been conducted by Faiz et al. [7]. A new methodology to evaluate the fracture attributes was devised by Ulhaq and Salehi [8]. The research work mentioned in this section is mostly based on subsurface image (electric and acoustic) logs and seismic data and is devoid of outcrop data analysis. Khairi Murat Range possessing a number of structural features offers a good opportunity to study fractures at the outcrop level. The objective of the study is to characterize the fracture properties of the outcropped sections in the Khairi Murat Range, by using the straight scanline and circle inventory methods. The research work in this study provides new avenues to understand natural fractures system, its role in providing the path to the fluid flow (groundwater or hydrocarbon) by determining fracture porosity, permeability and relation to *in situ* stress system in the study area.

2. Geology and Structure of the Area

2.1. Geology of the Area

The stratigraphic succession ranging in age from Early Eocene to Middle Pliocene is exposed in Khairi Murat Range and surrounding area [9]. The oldest exposed sequence is the Charrat Group consisting of Margalla Hill limestone, Chorgali Formation and Kuldana Formation having shallow marine, marine to continental palaeo-environments. Margalla Hill limestone consists of medium to thick bedded nodular limestone with subordinate marl and shale which is overlain by dolomitic, micritic and fossiliferous limestone with subordinate shales of Chorgali Formation [10-11]. Kuldana Formation having shallow marine, marine to continental palaeo-environments sparsely occurs in the study area.

Late Eocene to Oligocene strata is missing in the Potwar Fold Belt (PFB) due to non-deposition. The Early Eocene sequence is overlain unconformably by molasse of the Rawalpindi Group representing Miocene epoch. This group is represented by sandstone, siltstone and mudstone/shale sequences of Murree and Kamlial Formations and is widely exposed in and around the study area [12]. Siwalik Group, comprising the Chinji, Nagri and Dhok Pathan Formations of Mio-Pliocene overlies the Rawalpindi Group. Among the Formations of Siwalik Group, only Chinji Formation has good exposures at different localities in the study area. The clastics of the Rawalpindi and Siwalik Groups record the geodynamic process and episodic depositional history in the area [13]. The locations and details of the stratigraphic sequences of the study area are shown in Fig. 1 and Table 1.

2.2. Structure of the Area

The area lies in North Potwar Deformed Zone (NPDZ) and has imbricate, ramp-flat duplex structures, triangle zones, [14-17] and shortening of 55 km (55%) [1, 18, 19]. The area is greatly folded, faulted and fractured (Fig. 2a, b & c). The major structural elements in the area are the Main Boundary Thrust (MBT), Khairi Murat Thrust (KMT), Dhurnal back thrust, triangle zone, Khairi Murat anticline and Soan syncline (Fig. 2a). Along MBT, the Mesozoic-Cenozoic rock strata forming Margalla Hills has thrusted southwards over the Miocene sedimentary strata of Rawalpindi Group [3]. South of the MBT, the sedimentary strata comprising NPDZ has been imbricated by south directed thrusting with concurrent fault-related folding. The Khairi Murat Range constitutes the southern limit of the NPDZ and has been tectonically uplifted along south verging Khairi Murat Thrust (Fig. 2b). The south verging Khairi Murat thrust juxtaposes Eocene rock strata of the
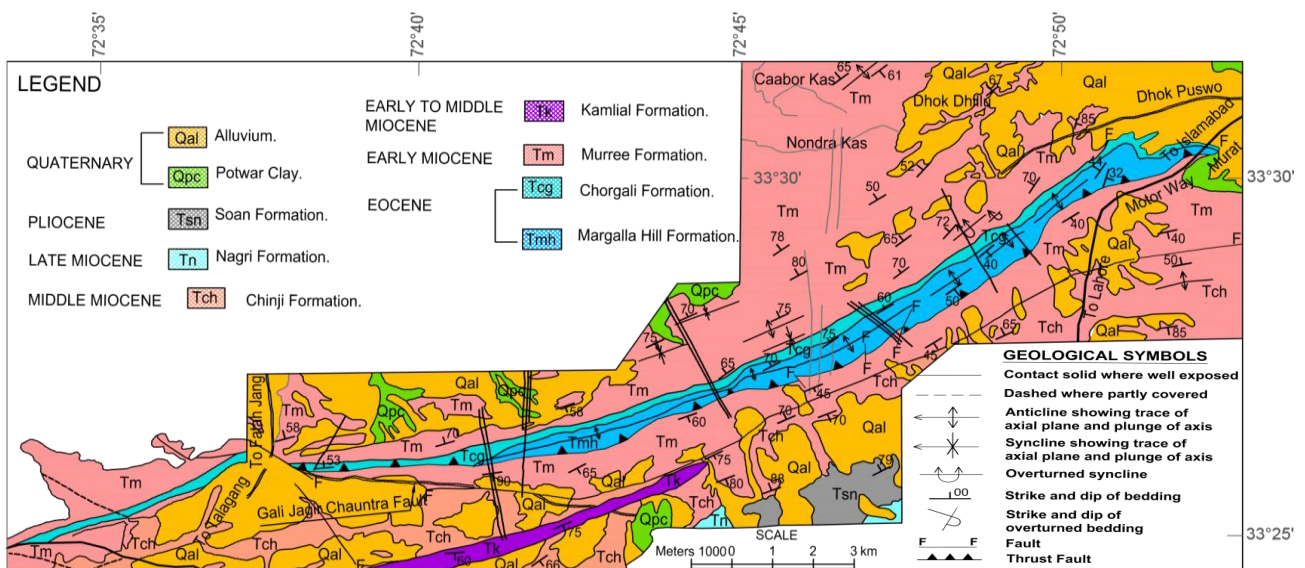
Fig. 1: Geological maps of the study area. The map contains litho-units and major structural features including regional scale lineaments (long black lines cutting across the main ridge). Litho-logical details of the geology (of each Formation) presented in this map can be viewed in Table 1 (modified after [9]).

Table 1: A Simplified stratigraphic column of the study area (derived from [12]).

Age	Formations		Lithology
Pliocene	Siwaliks	Soan Formation Dhok Pathan Formation Nagri Formation Chinji Formation	Clay, Silt, Gritty, Boulder Sandstone, Shale, Conglomerates. Sandstone, Siltstone, minor Marl Sandstone, Siltstone, Shale, Marl,
Miocene	Rawalpindi Group	Kamlial Formation Murree Formation	Reddish to light brown Sandstone. Siltstone, Mudstone Sandstone, Siltstone, Mudstone
Eocene	Charrat Group	Kuldana Formation Chorgali Formation	Shale, Sandstone, Limestone marl, clay Limestone (dolomitic), Shale
Eocene		Margalla Hill Limestone	Limestone, minor marl and shale

Khairi Murat Range against the Siwalik Group in the south (Fig. 1). The Siwalik sediments in the footwall of the Khairi Murat Thrust further to the south are thrusted over by a north facing passive roof thrust i.e. Dhurnal fault. This passive roof thrust at the surface shows underthrusting of Chinji Formation below Murree Formation along the northern flank of the Soan syncline (Fig. 2c). The area between Khairi Murat Thrust and passive back thrust (Dhurnal fault) forms a triangle zone [1, 3, 9, 15]. The triangle zone arrangement of faults is a common feature of the foreland basins throughout the world with associated tectonic wedges, sole thrusts and roof thrusts. This deeper level shortening has been accommodated by the development of a passive roof back thrust emanating from the tip of the southernmost ramp in the subsurface [17]. The strata along Khairi Murat Range show overturning behaviour with mesoscale sub-vertical folding due to associated transpression [14, 20]. In the footwall of Khairi Murat Thrust, Rawalpindi Group is exposed along the fault plane mostly dipping to the north. A number of anticlinal and synclinal structures are also present (Fig. 2a). Khairi Murat anticline is a major fold in the area. The Khairi Murat Range is cropped out in the result of the main anticlinal structure. The core of the anticline is composed of Margalla Hill limestone while Chorgali, Kuldana and Murree Formations are exposed on the northern limb of the anticline. Khairi Murat fault made the southern limb of anticline faulted [14]. The axis of the fold follows the general trend of the fault, i.e., NE-SW direction. Khairi Murat anticline has adjacent syncline which is clearly located between the Pari anticline and Khairi Murat overturned anticline. The rocks exposed in the northern part of the main ridge have been deformed into several anticlines and synclines named as Ratwal anticline, Ziarat syncline, Ratwal syncline and Ziarat anticline. These anticlinal and synclinal structural are locally present in the study area near Nondra Kas and Dhok Dhilu villages (Fig. 1).

3. Data Acquisition and Methodology

An area measuring 36×2 km was scanned for fracture sampling using straight scanline and circular scanline (circle inventory) methods. Straight scanline is a quick and systematic technique [21, 22]. Through the straight or linear scanline method, a wide range of fracture attributes can be captured [23]. In this method, measuring metric tape is placed on an outcrop to record attributes (i.e. orientation, spacing, aperture, intensity, fracture fills etc.) of all fractures that intersect the scanline [24, 25] (Fig. 3a). A GPS receptor is used to locate sampling stations in the field and later on, this data was used for preparing the map of the selected area. One of the advantages of using straight or linear scanlines over other methods of fracture sampling to characterize fracture heterogeneities is that straight scanlines are capable of capturing fractures variations recorded over longer tracts of outcrop (Fig. 3b). Care has been taken to avoid orientation bias in sampling by keeping scanline perpendicular to the strike of the fracture set as Priest [25] recommended that parallel and perpendicular to the bedding strike/dip should minimize this orientation bias. Circular scanline or circle inventory method is another effective tool for the estimation of fracture trace density and mean trace length (Fig. 3c). Trace density is defined as a mean number of trace centres per unit area $(1/m^2)$ and means trace length is defined as the length for individual fracture in a population (m) [26]. Circular scanlines or circular windows, together with circle-based estimators, provide time-efficient estimates for trace density and mean trace length. These methods are useful to eliminate orientation bias, censoring the outlier data and length bias with respect to measurements taken on a bedding plane. Circular scanlines are simply circles drawn on a rock surface, on a fracture trace map, or on a digital image.
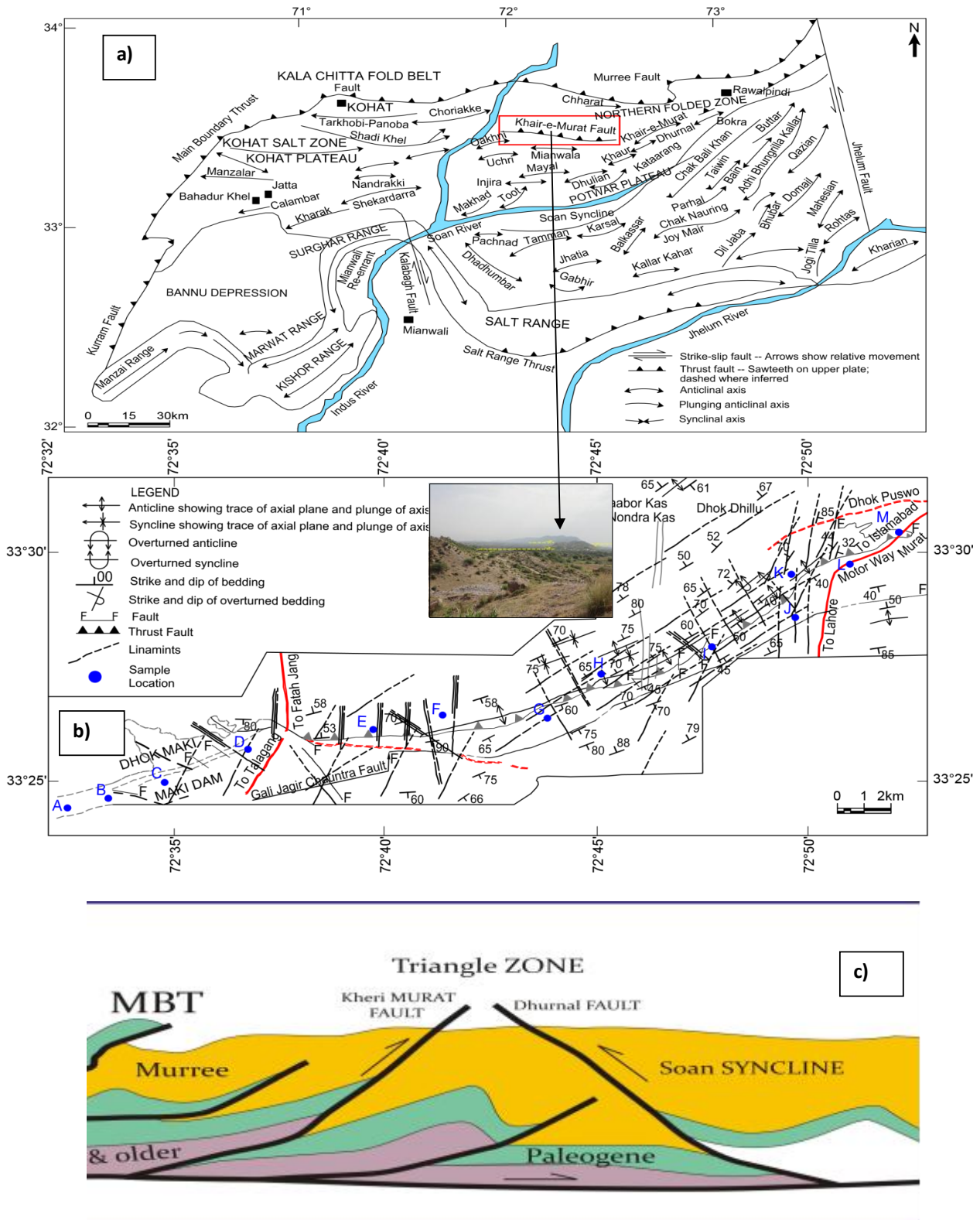
Fig. 2:   Maps showing a) regional structures, b) major structural elements of the study area. Long black freehand lines cutting across the ridge show lineaments observed from Satellite Imagery. Blue filled circles with capital alphabets show sampling locations. c) cartoon of cross-section indicating structural complexity and importance of the study. Photograph inside (b) shows a general view of Khairi Murat Range. Yellow arrows (on inset photograph) indicate Gali Jagir strike-slip fault, a prominent feature in the study area (Modified after [9]).

Fig. 3: Fractures at outcrops a) an example of scanline technique for measuring fractures from the outcrop. In most of the cases, these scanlines were placed perpendicular to the fracture trace to avoid sampling bias and using Terzaghi correction b) tract of outcrop (bedding face) showing fracture swarm and multiple fracture sets in single outcrop c) circle inventory for data collection d) view of fracture spacing exposed in the field. Co-author in the lower left of the photo (b) is for scale.

The terrain of the Khairi Murat Range selected for sampling and mostly covered with thick vegetation was very steep and rugged. Therefore, the best exposure of the fractures pavement was searched. About 2700 fractures were mapped at 106 stations through scanline method and 1260 individual fractures at 27 measuring sites through circular scanline method covering all the possible lithologic and structural domains throughout the area.

4. Fracture Characterization and Analyses

Fracture data from selected and approachable outcrops during field campaign through scanline sampling and circle inventory methods were collected. Out of the measured fracture properties; orientation, spacing between fracture to fracture along scanline at the intersection point (to evaluate fracture intensity or frequency) and aperture were taken to categorize fractures from sub-sets and sets to groups. Fracture porosities and permeabilities were estimated by using measured data in the field in the equations selected from literature referred in proceeding sections.

4.1. Fracture Orientation Analysis

Orientation distribution of rock fractures plays a vital role to evaluate the behaviour of rock with respect to stress trajectories identification, and influence reservoir fluid flow by controlling reservoir anisotropy and directional permeability [27]. The orientation of each rock fracture was

recorded at every scanline station. A large number of fracture orientation dataset has been analyzed and characterized. A wide dispersion in the orientation of fracture data has been observed.

It has been observed that the orientations are thoroughly spread in all four quadrants of a circle with close angles. For example, a number of fractures range from NS, N5°E, N7°E likewise N5°W and N7°W with minor distortion in the dip and strike angle. Similarly, some fractures fall in EW or N80°-85°W and N80°-85°E. The general trend of these fractures seems to be NS, EW and NW-SE. Some of them trending NE-SW while the others having strikes of ENE-WSW and WNW-ESE have been noted during the field survey. On the basis of a) similarities (strike and dip) between fractures and b) mode of mechanism or deformation (discussed in Section-5), the whole population has been grouped. Taking an interval angle of 25° ± 5°, all these fractures have been grouped into 8 sets and named them as Set-1, Set-2, Set-3, Set-4, Set-5, Set-6, Set-7 and Set-8 (Fig. 4 & Table 2). The frequency distribution (Fig. 4) of each set is performed using the open source 'Open plot software' [28]. Orientations of the fracture network are distributed into sets (groups) based on the "Right-Hand Rule" (RHR) method (Fig. 4). This method is an alternative form of presentation of azimuth or orientation of fractures in 360°circle. This method is a prerequisite input parameter of the software. Fig. 4 depicts the frequency of 8-fractures
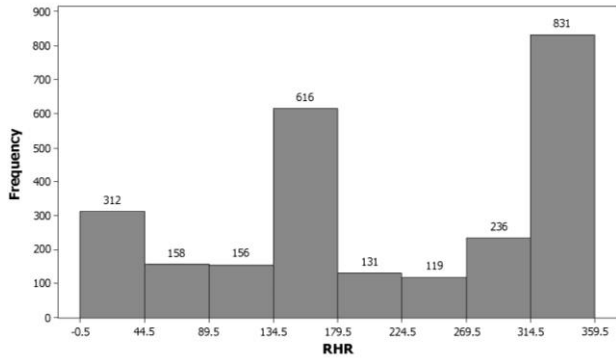
Fig. 4: Frequency Distribution of Orientation data of 8 fractures sets. Each bar represents a set. RHR denotes Right Hand Rule applied to characterize fracture frequency distribution. Numeric values on the top of each bar show number of fractures per fracture set.

sets. The fracture set striking in NW-SE direction (bracketed with bar 314° to 359°) is dominant throughout the study area. The least observed fracture set in the area is oriented in NE-SW (bracketed with bar 224° to 269°)

direction. Most of the places these two sets intersect each other making a conjugate relationship. This 1-D manual grouping of all measured population of fractures has been represented in the rose diagram (Fig. 5). The rose diagrams provide an overall view of the orientation of each fracture set in the fracture network within the scanned (measured) rock masses. Each diagram in the panel (Fig. 5) represents the directional data of the individual fracture set.

The purpose of statistical characterization and clustering of fracture orientations into sets is to determine the connectivity of the fracture network on the base of fracture intensity or density. From outcrop observations fracture network connectivity is difficult to attain. Outcrop data must be used to evaluate the statistical properties of the fracture network and establish a relationship between the statistics of network and connectivity. Statistical estimates of fracture orientation along with other parameters like spacing, aperture and length play a vital role to determine the connectivity of the fracture network. To describe the connectivity of fracture is beyond the scope of this paper.

Table 2: Differentiation of fracture sets based on orientation data at 25° intervals. Azimuth (strike) is based on RHR (Right-Hand-Rule).

Data Set	Strike	Azimuth	Fracture No.	Data Set	Strike	Azimuth	Fracture No.
Set-1	N10E	10	70	Set-2	N85E	85	3
Set-1	N10W	350	223	Set-2	N85W	275	1
Set-1	N12W	348	2	Set-3	N50E	50	7
Set-1	N15E	15	11	Set-3	N55E	55	3
Set-1	N15W	345	185	Set-3	N60E	60	70
Set-1	N16W	344	1	Set-3	N65E	65	44
Set-1	N17W	343	1	Set-4	N25E	25	24
Set-1	N18W	342	14	Set-4	N30E	30	28
Set-1	N20E	20	42	Set-4	N35E	35	47
Set-1	N20W	340	168	Set-5	N40E	40	68
Set-1	N22E	22	1	Set-5	N45E	45	23
Set-1	N22W	338	15	Set-6	N48W	312	2
Set-1	N4W	356	1	Set-6	N50W	310	101
Set-1	N5E	5	6	Set-6	N55W	55	56
Set-1	N5W	355	6	Set-6	N60W	300	42
Set-1	N7W	353	2	Set-6	N65W	295	25
Set-1	N-S	0	124	Set-6	N68W	292	1
Set-2	E-W	90	101	Set-7	N40W	320	128
Set-2	N70E	70	73	Set-7	N43W	317	2
Set-2	N70W	290	6	Set-7	N45W	315	63
Set-2	N72W	288	1	Set-8	N25W	335	99
Set-2	N73W	287	1	Set-8	N27W	333	2
Set-2	N75E	75	31	Set-8	N28W	332	16
Set-2	N75W	285	29	Set-8	N30W	330	271
Set-2	N78W	282	1	Set-8	N32W	328	2
Set-2	N80E	80	45	Set-8	N34W	326	2
Set-2	N80W	280	26	Set-8	N35W	325	105

4.2 Fracture Spacing Analysis

Fracture spacing is defined as the linear distance (perpendicular to strike) between two fractures that intersect sampling line i.e. scanline. In other words, the spacing is a distance between consecutive intersections of two fractures of the same set with the sample line [29-31] as shown in Fig. 3d. Fracture spacing depends upon mechanical property contrast between rock beds and correlates with mechanical bed thickness [31]. We ignore this property and measure fracture spacing from maximum possible exposed lithologies of having good fracture trace exposures in the study area.

Fracture spacing data has been collected along scanlines at 107 stations covering more than 36×2 km area along Khairi Murat Range. To eliminate sampling bias, fracture spacing from dataset requires a correction [32]:

$$D = D'\sin(\alpha) \qquad (1)$$

to convert the apparent spacing D' measured along a scanline to true fracture spacing D. Values of "α" refer to the angle of scanline relative to the mean fracture orientation (Fig. 6).

After applying a correction (equation-1) on fracture spacing, values of fracture frequency and average fracture spacing can be calculated. The total number of fractures along the unit length of scanline denotes fracture frequency (units of inverse length, L^{-1}) while fracture spacing (units of length, L) is simply the inverse of fracture frequency. An average spacing frequency of the measured fractures along the scanline is estimated as 8 fracture/m which is also termed as closely spaced fractures.
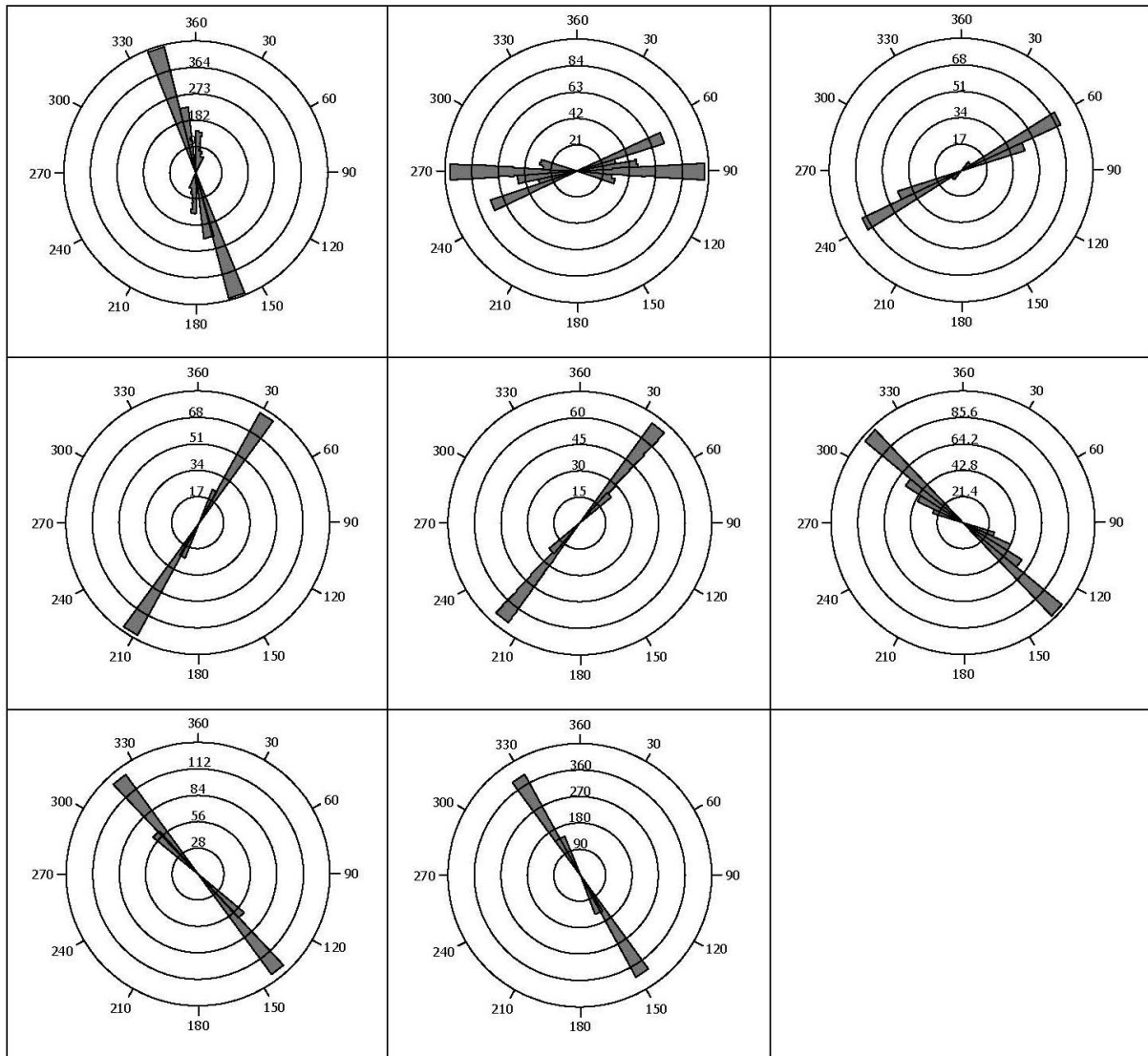
Fig. 5: Rose diagram of fracture sets observed in the study area. The panel is composed of eight fracture sets. Each fracture set has its own independent orientation (strike & dip). The panel displays fractures sets set-1 to set-8 starting from upper left to right up to down last one.
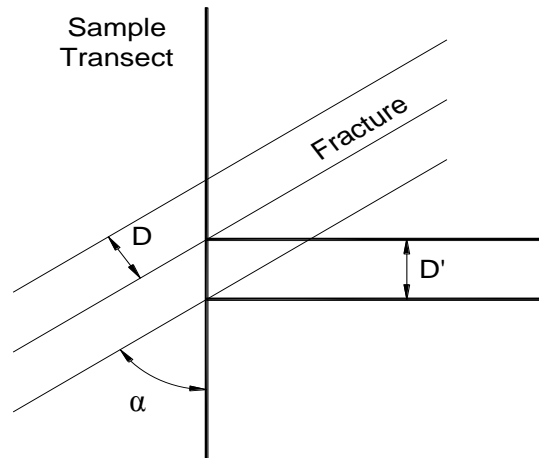
Fig. 6:   Illustration of application of Terzaghi correction to the spacing data. See text for detail (after [32])
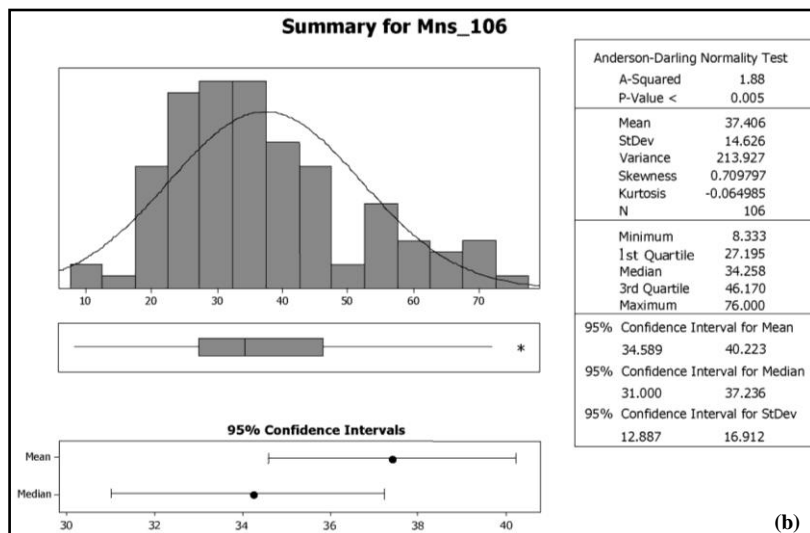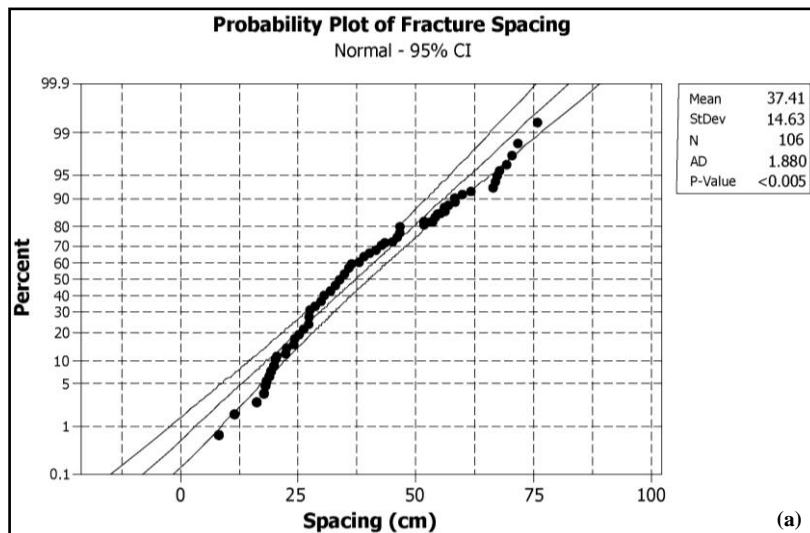
Fig. 7:   Spacing distribution of outcrop fracture data a) probability frequency plot shows the general trend of variability in spacing data which favours using log-normal distribution b) shows log-Normal distribution curve of spacing along with a statistical table containing analysis information. In the title of (b) Mns_6 means "maximum number of observation i.e.106".

Fracture spacing data along linear or straight scanline (sampling bias is minimized by applying Terzaghi correction, equation (1) from a large number of outcrops encompassing all type of fractures that touch the sampling line has been collected. Statistical analysis on the basis of histogram indicates that the distribution of fracture spacing follows positive skewness with the platykurtic curve as the results are given in the data table of Fig. 7. Probability density plot also depicts the variability of data deviating from a normal distribution (Fig. 7a). The numerical values presented in Fig. 7b are indicative of that the data is positively skewed and platykurtic (value of kurtosis is < 3) with mean value of 37.40 and P-value (level of significance) less than 0.5. Due to positively skewed and platykurtic nature of fracture spacing data and to eliminate the variability in observations taken from natural data, we chose a lognormal distribution. The data in Fig. 7 shows that the maximum observations of the data lie in the left side (or spacing values of 20 cm to 45 cm are concentrated in the centre of the histogram) while the spacing ranges from 50 cm to 70 cm are right-tailed. It is inferred that the fractures are generally closely spaced whereas largely spaced fractures are of a lesser frequency and sparsely present in the area. As mentioned by Cosgrove [33], the negative value of kurtosis shows the spatial variation of data set regarding more than one fracture sets spread out in the sampled area.

4.3 Fracture Aperture Analysis

Aperture is defined as the width of crack or the perpendicular distance between the adjacent surface of fracture plane in which the intervening space is filled with air or fluid [29, 33, 34, 35]. Generally, the aperture is quite difficult to define in term of true width because the mechanical properties of rock masses and propagation mechanism of fracture opening also affect the aperture opening size. Aperture is one of the most significant properties of rock masses which commonly have small (tight) aperture in the subsurface. Its size ranges from microscopic to macroscopic level depending on whether the opening is under stressed (e.g. in situ confining pressure or overburden) or non-stressed conditions. Aperture has a broad spectrum of applications in almost all disciplines of earth sciences. Analysis and determination of its role have great importance. Fracture frequency and aperture data from the bedrock exposures in Khairi Murat Range has been acquired during field studies using vernier calliper (for precise measurements) and feeler gauge (an engineering tool, consists of a number of small lengths of steel bars (blades) of different thickness with measurements marked on each piece to measure gap widths). Outcrop measurements of fracture frequency and aperture distribution at each station (of 107 scanline measuring stations) were taken. The frequency histogram of the fracture aperture data represents normal distribution (Fig. 8). A bell-shaped curve of a normal distribution has been

superimposed over the observed data. Generally, the histogram of real data does not look like a perfectly normal distribution. The dispersion parameter is the standard deviation which is in our case is 0.21. The maximum aperture size of individual fracture is 3mm. Cumulative values of the aperture in all fracture sets observed within a circle vary in range from 1.1 cm to 13.4 cm (Table 3). The flatness of the bell curve represents that the data are spread far apart. The Gap and flat behaviour (Fig. 8) also shows that the data constitute spatial variation in data measurements due to lithologic and structural domains contrast effects. The negative value of kurtosis also is an indication of variability and multi-diversity in rock fracture network.

Observation Stations=107
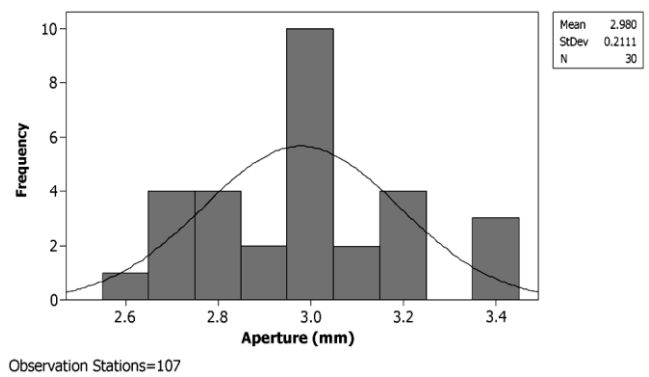
Fig. 8: Histogram showing frequency of fracture aperture. Statistical distribution curve shows the best-fit distribution information of aperture data.

4.4 Fracture Density Analysis

The density of fractures depends on 1) mechanical property of rock unit, 2) bed thickness, 3) structural position and 4) strength of stress [35]. Fracture density is described as the summation of the occurrence of a total number of fractures (irrespective of fracture sets) at a sampling station. Since the sampling of the fractures is carried out by the unit radius of the circle (circle inventory method), therefore, the total length of all fractures (within a circle of specified radius) divided by the area of the circle is defined as fracture density. Mathematically it is written as:

$$Pf = {}^{L}\!/_{\pi r^2} \qquad (2)$$

Where

Pf = Fracture density

L = Cumulative length of all fractures

r = radius of the inventory circle

Unit of density is expressed as length/area (e.g., cm/cm^2, m/m^2, km/km^2). In general, the value of density is expressed in the reciprocal form (i.e. cm^{-1}, m^{-1} and km^{-1}). Density values are used in many applied studies. We use the obtained density values (Table 3) to determine the fracture-induced permeability in the study area.

Using circular inventory method, a number of 27 sampling stations were selected. A symmetrical circle (having equal radius throughout the sampling stations to maintain data precision, i.e., 1 m, except sampling station No. 27 where excellent outcrop face consisting of good exposure of fractures were observed), at each station, was drawn on bedding surface of exposed outcrop. The maximum density 0.22 cm^{-1} is observed at inventory circle No. C12 (Table 3). At this station, two fracture sets having strikes N30°W and N60°E have been identified and measured all particulars of both the sets. While at station C5, one set trending N30°W and the second with N25°E attitude give minimum value of density, i.e., 0.05 cm^{-1}. This discrepancy is probably related to rock behaviour towards external forces. Analysis of the data indicates that variation in the values of density within the same set is due to 1) mechanical layering effect 2) intensive deformation changing effect and 3) position of the structure. It is generally expected that laminated (thin) strata show a higher density of fracture as compared to massive strata [6].

4.5 Fracture Porosity Analysis

Interconnectivity of preexisting pores in rock mass by fracturing induced by tectonic stresses is called fracture porosity. This definition of fracture porosity may not be confused with the academic definition of matrix porosity. It is a kind of secondary porosity and more compatible with the term of transmissivity of the fractured medium. Fracture porosity in rock masses generally depends upon primary attributes of fractures i.e. density, aperture and spacing. The data of all these fractures properties were collected in the study area by using circle inventory method. To estimate fracture porosity for the study area, the following mathematical equation has been applied [4, 36, 37].

$$\text{Porosity} = \left(1/_A\right) \sum_{i=1}^{N}(L_i \times W_i) \qquad (3)$$

Where

i: is the index to designate each fracture in the inventory circle

Li: is the length of ith fracture

Wi: is the width of the ith fracture.

N: is the number of fractures in the inventory circle

A: is the area of inventory circle

The results presented in Table 3, depict porosity values ranging from 0.06% to 2.30% which is in accordance with the values reported in previous literature [4, 6]. The porosity of the lithological Formations exposed at different locations (other than study area) in Potwar region, that has been recorded in the previous literature ranges from 1% to 24% with an average value of 4% [4, 6]. Further, they found that fracture porosity ranges from 2% to 8% (for Chorgali Formation) and up to 6.5% for Sakesar Limestone [4, 6, 37]. Shah et al. [36] reported that porosity values over

Jabbar anticline (of Dhok Pathan Formation) ranges from 0.6% to 2%.

4.6 Fracture Permeability Analysis

Permeability is the measure of ease of fluid flow through an interconnected medium or connected pore spaces in the rock mass. Fracture surfaces (particularly of planar nature) provide an easy way for water transmission in the fracture system. The easy transmission of water through rock mass is referred to as its permeability or hydraulic conductivity. The hydraulic conductivity is determined by the permeability of the rock matrix and of the fractures. It is generally accepted that the matrix conductivity of the rock mass is negligible as the naturally occurring fractures in the rock have considerably greater conductivity. Fractures along with their physical parameters have a substantial influence on the permeability of the unit medium. For example, less than 0.0002 inches (0.000508 cm) aperture is sufficient for fluid flow [4]: means precise measurements of the fracture width (aperture) are very significant in calculating the permeability of the sampled site. To estimate the fracture-induced permeability, the following formula has been used:

$$K = (3.5 \times 10^8)\left(1/_A\right)\sum_{i=1}^{N}(L_i \times W_i^3) \qquad (4)$$

where

K: permeability in Darcy (D)

i: index to designate each fracture in inventory circle

N: number of fractures in the inventory circle

Wi: width of the ith fracture

A: area of the inventory circle and

3.5×10^8: a factor to convert magnitude into Darcy (D)

A Monte Carle technique has been used to calculate the permeability using data input parameters obtained from field observations. Our research work contains permeability values ranging from 0.236×10^8 D to 1446.1×10^8 D. We found that the results have some anomalous values i.e. 1037×10^8 D and 446×10^8 D (Table 3) of the permeability estimates. Ulhaq and Salehi [8], used the equation:

$$K_f = C\left(\frac{A^3}{S}\right)E + 9/_{12} \qquad (5)$$

Where

K_f : fracture permeability in mD (miliDarcy)

S : fracture spacing in m

A : aperture in cm

E : Elastic moduli

C: constant

and estimated 76.8 md fracture permeability for natural and open single fracture which has a fracture aperture of 0.02 cm and 0.00011% fracture porosity. A 20 m fractured zone has contributed (100%) 1977 bpd (billion per day) in

production and believed to have 729.6 md estimated permeability [8].

Using the equation:

$$K_f = k \cdot \frac{h}{hf} + \left(\frac{h}{hf} - 1\right) k \qquad (6)$$

Where

K_f : fracture permeability in mD (miliDarcy)

hf : fracture aperture in mm

k : average permeability and

h : hight or thickness

Ulhaq and Salehi [8] obtained estimated permeability of 751.3 md for 20 m thick open fracture zone. Keeping in

view the above scenario, our estimation of fracture permeability tabulated in Table 3 is consistent with the permeability estimation values in the published research work with more or less fewer variations. We are of the opinion that some of the abnormal/high values of permeability represent the occurrence of fisher, shear and fault damage zones, swarms of fractures with open apertures which exist in the area as a result of tectonic deformation. Another justification in the estimation of permeability values is that the samples C9 and C13 are measured in structurally disturb zones (on the crest of anticline) where fractures have aperture values of 12.6 cm and 13.4 cm, respectively.

Table 3: Fracture density, porosity and permeability measured from outcrops of Khairi Murat area. The data are collected through circle inventory method.

Circle No.	Northing	Easting	T. Length* (cm)	T. Aperture** (cm)	Density (cm⁻¹)	Porosity (%)	Permeability (1x10⁸) D	Area*** (cm²)
C1	33 10 16 N	072 52 31 E	871	1.85	0.11	0.21	2.46	7850
C2	33-28-27 N	072-50-12 E	868	6.7	0.11	0.74	116.40	7850
C3	33-28-28 N	072-50-14 E	893	6.1	0.11	0.69	90.37	7850
C4	33-30-00 N	072-52-05 E	702	1.4	0.09	0.13	0.86	7850
C5	33-27-46 N	072-49-48 E	398	1.1	0.05	0.06	0.24	7850
C6	33-24-52 N	072-33-05 E	765	3.7	0.10	0.36	17.28	7850
C7	33-26-32 N	072-37-39 E	959	3.9	0.12	0.48	25.36	7850
C8	33-26-47 N	072-38-15 E	764	2.2	0.10	0.21	3.63	7850
C9	33 25 58 N	072 39 02 E	1163	12.6	0.15	1.87	1037.27	7850
C10	33 25 59 N	072 39 08 E	781	5.5	0.10	0.55	57.93	7850
C11	33 25 59 N	072 38 08 E	771	3.5	0.10	0.34	14.74	7850
C12	33 25 58 N	072 39 07 E	1706	5.9	0.22	1.28	156.22	7850
C13	33 25 58 N	072 39 07 E	1348	13.4	0.17	2.30	1446.11	7850
C14	33 25 58 N	072 39 07 E	505	4.75	0.06	0.31	24.13	7850
C15	33 25 58 N	072 39 08 E	1238	6	0.16	0.95	119.23	7850
C16	33 25 58 N	072 39 08 E	1422	4.8	0.18	0.87	70.12	7850
C17	33 25 59 N	072 39 07 E	1184	4.9	0.15	0.74	62.11	7850
C18	33 25 59 N	072 39 07 E	966	3.7	0.12	0.46	21.82	7850
C19	33 26 18 N	072 41 02 E	733	3.1	0.09	0.29	9.74	7850
C20	33 26 19 N	072 41 05 E	404	2.1	0.05	0.11	1.67	7850
C21	33 26 09 N	072 41 09 E	916	5.1	0.12	0.60	54.18	7850
C22	33 26 13 N	072 41 07 E	407	1.8	0.05	0.09	1.06	7850
C23	33 26 59 N	072 34 06 E	974	10.6	0.12	1.32	517.22	7850
C24	33 25 13 N	072 34 58 E	308	2	0.04	0.08	1.10	7850
C25	33 25 13 N	072 34 58 E	690	3.9	0.09	0.34	18.25	7850
C26	33 25 59 N	072 39 07 E	1176	5.1	0.15	0.76	69.55	7850
C27	33 25 25 N	072 35 59 E	2150	8.4	0.07	0.58	142.04	31400

*Total length of all fracture traces measured in a circle

**Total aperture of all fractures observed in a circle

*** Area of a circle is calculated by πr^2

5. Fracture Types and their Relationship with Tectonics

Three types of fractures have been observed from selected outcrops during a field survey in the study area, which can be classified as; a) opening mode fractures, b) shear fractures and c) mixed mode fractures or hybrid fractures [38]. NW-SE trending fracture sets (trend ranges from N5°W to N20°W are opening mode fractures. These are vertical to sub-vertical, regionally extended (of regional scale; can be mapped in the surrounding of the study area) and nearly normal to the general strike of the strata and parallel to the direction of principal compressive stress (regional tectonic stress). The surface planes of the fracture set have imprints of hackle and plumose structures. The hackle and plumose structures are the morphological features of the feather-like pattern on the walls of the fractures or joints. Their presence distinguishes extension joints from shear fractures. These imprints are well expressed in mudstone of Murree Formation near Dhok Maiki, Gali Jagir area. These are present throughout the study area. The NE-SW trending fracture set is another dominant set in the area that makes a conjugate relationship with NW-SE striking fractures; possess slickenlines and groves on the surface of the fracture walls. From the slickensided surfaces of the fracture planes, the direction of the movement has been measured. These have equal or less than 45° angle with the axes of maximum principal stress. At many places, evidence of oblique slip has also been recorded during the field survey. Oblique-slip (by observing striations on the walls of fracture) is the indication of the development of mixed mode fractures which are also known as Mode-III fracture or tearing mode fractures. In this fracturing, shear stress acts parallel to the plane of crack or fracture. Near Dhok Maiki in the vicinity of Gali Jagir strike-slip fault, an array of oblique slip fracture sets at different locations has been observed. WNW-ESE fracture sets represent oblique slip features. To establish an abutting relationship between these and another such type of fractures is difficult due to multi-phase tectonics developing multiple structural events.

6. Discussion and Conclusion

The estimation and evaluation of fracture properties i.e. orientation, density, spacing, aperture, porosity and permeability are one of the effective methods to characterize the fracture system. The numerical values of these properties are the basic input parameters of fluid flow modelling, to improve the understanding of geomechanics and geotechnical studies. The study area although has limited rock exposure of outcrops (due to thick vegetation and cover with erosion material), exhibits good imprints of natural fractures. Orientation data are interpreted as the main link to the directional character of fracture connectivity. The spatial occurrence of fracture population has been characterized and grouped into 8 sets. In order to constrict the angular diversity in the directional trend of the individual fractures, the angle interval has been fixed at 25° with ± 5° variation. Fracture set-1, NW-trending (N 5°W to N 20°W) dominates over the categorized population of fracture network followed by fracture set-8 (N20°W to N35°W), the second dominant fracture set in the study area. The orientation pattern of set-1, set-6, set-7 and set-8 is consistent with the structural orientations recorded in outcrops of the area in that NE trending structures are dominant. The general trend of the fracture network has been illustrated in rose diagrams.

The distribution of fracture spacing, length and aperture contribute to determining the possible interconnectivity of the natural fracture system. The fractures are closely spaced (average /mean spacing is 8 fractures/m), have a considerable length (length varies from 308 cm to 2150 cm in a circular area of 1 m dia, except sample C27 is of 3 m dia) and contain aperture value up to 13.4 cm. Generally, fracture frequency is dependent on the geometry of the fractures, the scanline intersects and the orientation of the sampling line. By applying Terzaghi correction, fracture spacing gains the independent identity of the fracture system and does not rely solely on the orientation of the fracture sets.

The orientation of fractures and spacing along with aperture affect fluid flow in the sub-surface. For example, in isotropic fracture systems, the fluid percolation threshold is mainly dependent on fracture size, but this is not true for anisotropic (azimuthal variation) systems. Thus the robust measures of fracture spacing, orientation, and aperture and strike anisotropy have great concern with the disciplines of hydrocarbon production, hydrogeology, waste disposal or storage and many rock engineering projects The fracture density, porosity and permeability values have been calculated from data collected from field observations. Measured values of these properties ranges from 0.05 cm^{-1} to 0.217 cm^{-1}, 0.24% to 2.30% and 0.24×10^8 D to 1446.114×10^8 D respectively. The fluctuations in the results are suggested to be related to the proximity to the faults, lineaments, structural position and intensity of stress towards strain. In addition, the anomalous values of permeability are the indications of a significant flaw or bug in equations which are used to calculate permeability. Rather censoring the data, we recorded the error which is not mentioned in the previous literature. Fracture parametric distributions and their statistical evaluation give insight and basic parametric input values for the development of hydro litho-structural model and enhancement of hydrocarbon productivity in future.

References

[1] T.M. Jaswal, R.J. Lillie and R.D. Lawrence, "Structure and evolution of the Northern Potwar deformed zone, Pakistan", AAPG Bulletin, vol. 81, no. 2, pp. 308-328, 1997.

[2] M. Iqbal and D. Bannert, "Structural observation of the Margalla Hills, Pakistan and the Nature of the Main Boundary Thrust", Pak. J. Hydrocarb Res, vol. 10, pp. 41-53, 1998

[3] T.M. Jaswal, "Triangle zone in the himalayan foreland, North Pakistan", Himalaya and Tibet: mountain roots to mountain tops, pp. 328-275, 1999.

[4] W.A.K. Jadoon, B.A. Shami and I.A. Abbasi, "Fracture analysis of Khaur anticline and its implications on subsurface fracture system", PAPG-SPE Annual Technical Conference and Oil Show, 3-5 October, Islamabad, Pakistan, pp. 235-250, 2003.

[5] M.S.K. Jadoon, I.A.K. Jadoon, A.H. Bhatti and A. Ali, "Fracture Characterization and Their Impact on the Field Development", SPE/PAPG Annual Technical Conference, Society of Petroleum Engineers, 2005.

[6] I.A.K. Jadoon, K.M. Bhatti, F.I. Siddiqui, M.S.K. Jadoon, S.R.H. Gilani and M. Afzal, "Subsurface fracture analysis in carbonate reservoirs: Kohat/Potwar Plateau, north Pakistan", SPE/PAPG Annual Technical Conference.Society of Petroleum Engineers, 2005.

[7] M.I. Faiz, S. Ahmad, A.J. Malik, F. Ali and M.I. Khan, "Structural analysis of Sakesar limestone exposed along the Surghar anticline: Implications for assessing secondary porosity and permeability for its potential as hydrocarbon reservoir", PAPG/SPE Annual Tech.Conf, Islamabad, pp.187-192, 2010.

[8] S. Ulhaq and F. Salehi, "A Unique Methodology to Estimate Fracture Permeability in Naturally Fractured Reservoirs (NFR)", SPE/PAPG Annual Technical Conference, Society of Petroleum Engineers, Jan 2010.

[9] H. Jurgan and G. Abbas,"On the Chorgali Formation at the Type Locality", Pak. J. Hydrocarb. Res., vol. 3, pp. 35-45, 1991.

[10] S.M. Kamran, M.S. Khan, M.I. Siddiqui, and M.H. Munir, "Micropalaeontology and depositional environment of the early eocene Margalla Hill limestone and Chorgali formation of the Khairi Murat Range, Potwar Basin, Pakistan", Pak. J. Hydrocarb. Res., vol. 16, pp. 51-57, 2006

[11] S.M.I. Shah, "Stratigraphy of Pakistan", Memoirs vol. 12, Geological Survey of Pakistn, 1977.

[12] A.H. Kazmi, and M.Q. Jan, "Geology and tectonics of Pakistan", Graphic Publishers, Karachi, pp. 56-76, 1997.

[13] I.A.K. Jadoon and W. Frisch, "Hinterland-divergent tectonic wedge below Riwat Thrust, Himalayan Foreland, Pakistan: Implication for hydrocarbon exploration", AAPG Bulletin, vol. 81 no. 3 pp. 438-448, 1997

[14] I.A.K. Jadoon, W. Frisch, A. Kemal and T.M. Jaswal, "Thrust Geometries and Kinematics in the Himalayan Foreland (North Potwar Deformed Zone), North Pakistan", Geologische Rundschau, vol. 86, no. 1, pp. 120-131, 1997.

[15] I.A.K. Jadoon, W. Frisch and M.S.K. Jadoon, "Structural traps and hydrocarbon exploration in the Salt Range/Potwar Plateau, North Pakistan", SPE Annual Technical Conference, Islamabad, pp. 69-82, 2008.

[16] I.A.K. Jadoon, M. Hinderer, B. Wazir, R. Yousaf, S. Bahadar, M. Hassan and S. Jadoon, "Structural Styles, hydrocarbon prospects and potential in the Salt Range and Potwar Plateau, North Pakistan", Arabian Journal of Geosciences, vol. 8, no. 7, pp. 5111-5125, 2015.

[17] D.M. Baker, R.J. Lillie, R.S. Yeats, G.D. Johnson, M. Yousuf and A.S.H. Zaman, "Development of the Himalayan frontal thrust zone: Salt Range, Pakistan", Geology, vol. 16, no. 1, pp. 3-7, 1988.

[18] E.S. Pennock, R.J. Lillie, A.S.H. Zaman and M. Yousaf, "Structural interpretation of seismic reflection data from Eastern Salt Range and Potwar Plateau, Pakistan", AAPG Bulletin, vol. 73, no. 7, pp. 841-857, 1989.

[19] T.M. Jaswal, "Triangle zone in the Himalayan Foreland, North Pakistan", Himalaya and Tibet: Mountain roots to mountain tops, pp. 328-275, 1999.

[20] P.R. La Pointe and J.A. Hudson, "Characterization and interpretation of rock mass joint Patterns", Int. J. Rock Mech. Min. Sci. & Geomech., Abstract, vol. 22, No. 5, p. 146, 1985.

[21] D.C.P. Peacock, S.D. Harris, and M. Mauldon, "Use of curved scanlines and boreholes to predict fracture frequencies", Journal of Structural Geology, vol. 25, no. 1, 109-119, 2003.

[22] H. Watkins, C.E. Bond, D. Healy and R.W.H. Butler, "Appraisal of fracture sampling methods and a new workflow to characterize heterogeneous fracture networks at outcrop", Journal of Structural Geology, vol. 72, pp. 67-82, 2015.

[23] S.D. Priest and J.A. Hudson, "Estimation of discontinuity spacing and trace length using scanline surveys", Int. J. Rock Mech. Min. Sci. & Geomech., Abstracts, vol. 18, no. 3, pp. 183-197, 1981.

[24] G.B. Baecher, "Progressively censored sampling of rock joint traces", J. Int. Assoc. Math. Geol., vol. 12, no. 1, pp. 33-40, 1980.

[25] S.D. Priest, "Discontinuity analysis for rock engineering", Springer Science & Business Media, 2012.

[26] N.H. Tran, Z. Chen and S.S. Rahman, "Practical application of hybrid modelling to naturally fractured reservoirs", Petroleum Science and Technology, vol. 25, no. 10, pp.1263-1277, 2007.

[27] A. El-Naqa, "The hydraulic conductivity of the fractures intersecting Cambrian sandstone rock masses, Central Jordan", Environmental Geology, vol. 40, no. 8, pp. 973-982, 2001.

[28] S. Tavani, P. Arbues, M. Snidero, N. Carrera, and J.A. Muñoz, "Open Plot Project: An open-source toolkit for 3-D structural data analysis", Solid Earth, vol. 2, no. 1, p. 53, 2011.

[29] H. Alizadeh, B. Rahimi and M.F. Golyan", Statistical and fractal analysis of the fractures in Derakht-e-Bid Tonalite, West of Mashhad, North-East Iran", 1st Int. Appl. Geol. Congress, 26-28 April, 2010.

[30] Y. Tan, T. Johnston and T. Engelder, "The concept of joint saturation and its application", AAPG Bulletin, vol. 98, no. 11, pp. 2347-2364, 2014.

[31] D.M. Reeves, R. Parashar and Y. Zhang, "Hydrogeologic characterization of fractured rock masses intended for disposal of radioactive waste", Radioactive Waste. InTech, 2012.

[32] R.D. Terzaghi, "Sources of error in joint surveys", Geotechnique, vol. 15, no. 3, pp. 287-304, 1965.

[33] J.W. Cosgrove, W. John and T. Engelder, eds. "The initiation, propagation, and arrest of joints and other fractures", Geological Society of London, 2004.

[34] A. Aydin, "ISRM suggested method for determination of the Schmidt hammer rebound hardness: revised version", The ISRM Suggested Methods for Rock Characterization, Testing and Monitoring: 2007-2014, Springer, Cham- pp. 25-33, 2008.

[35] B. Singhal, B. Saran and R.P. Gupta, "Applied hydrogeology of fractured rocks", Springer Science & Business Media, 2010.

[36] S.M.A. Shah, A. Hafeez and R.N. Khan, "Fracture analysis of the Dhok Pathan Formation at the Eastern limb of the Jabbar anticline, northeastern Potwar, district Rawalpindi", Geol. Bull. Punjab Univ. vol. 43, pp.27-34, 2008.

[37] A.H. Baitu, R.A. Sheikh, A.J. Deo, A.U. Rehman and A. Wahab, "Fracture analysis of Eocene Sakesar limestone at Mardwal Anticline, Soan-Sakesar valley, Western part of Central Salt Range, District Khushab, Pakistan", Geol. Bull. Punjab Univ. vol. 43, pp.121-130, 2008.

[38] D.C.P. Peacock, C.W. Nixon, A. Rotevatn, D.J. Sanderson and L.F. Zuluaga, "Glossary of fault and other fracture networks", Journal of Structural Geology vol. 92, pp.12-29, 2016.